Constellation Design for Multiuser Non-Coherent Massive SIMO based on DMPSK Modulation

Manuel J. Lopez-Morales, *Student Member, IEEE*, Kun Chen-Hu, *Member, IEEE*, Ana Garcia-Armada, *Senior Member, IEEE*, Octavia A. Dobre, *Fellow, IEEE*

***Abstract*—Non-coherent (NC) schemes combined with massive antenna arrays are proposed to replace traditional coherent schemes in scenarios which require an excessive number of reference signals, since NC approaches avoid channel estimation and equalization. Differential M-ary phase shift keying is one of the most appealing NC schemes due to its implementation simplicity in realistic scenarios. However, the analytical constellation design for multiuser scenarios is intractable, as discussed in this paper. We propose to solve this problem by using optimization techniques relying on evolutionary computation. We design two approaches, namely Gaussian-approximated optimization and Monte-Carlo based optimization. They can provide both individual constellations for each user equipment and a bit mapping policy to minimize the bit error rate. We perform a complexity analysis and propose strategies for its reduction. We propose a set of constellations for different number of users and constellation sizes, and evaluate the link-level performance of some illustrative examples to verify that our solutions outperforms the existing ones. Finally, we show via simulations that NC outperforms the coherent schemes in high mobility and/or low signal-to-noise ratio scenarios.**

***Index Terms*—Non-coherent, massive multiple-input-multiple output (MIMO), differential modulation, constellation design, evolutionary computation.**

I. Introduction

In recent years, a great variety of heterogeneous services and applications has emerged. Consequently, the fifth generation (5G) of mobile communications has developed a new-radio [1], which supports different service classes. Furthermore, it is desirable to deploy these services in new scenarios with very stringent constraints, such as high mobility [2] and low signal-to-noise ratio (SNR) [3], which were not achieved in previous mobile communications generations.

The coherent detection approach is widely adopted in many communication systems, where accurate channel state information (CSI) is required to mitigate the channel effects. For this, reference signals must be transmitted, at the expense of producing signaling overhead. Additionally, the coherent scheme requires an acceptable SNR to obtain an accurate enough CSI; otherwise, the equalized symbols suffer from additional interference [4], [5]. In traditional scenarios, the overhead can be constrained if the channel is considered quasi-static and the number of antennas is not very large. Otherwise, for massive multiple-input multiple-output (MIMO) [6], numerous reference signals are required, especially in a multiuser (MU) massive MIMO scenario with reduced or moderate mobility. In general, the coherent scheme is not recommendable in high-mobility and/or short packet communications, since it requires a large number of reference signals to effectively track the channel variations, severely reducing the effective data-rate [4], [7].

Non-coherent (NC) schemes combined with massive MIMO are able to transmit information without CSI knowledge, with the same asymptotic performance as coherent schemes [4]. Thus, the reference signals are avoided and the complexity of transceivers is reduced. Additionally, [7] showed that the NC detection can provide an acceptable performance in very fast time-varying scenarios, while the coherent scheme fails. In the literature, some works targeted the uplink (UL) based on the spatial diversity provided by the high number of antennas at the base station (BS) [8]–[10], while others focused on using beamspace processing [11], [12]. An NC scheme based on differential M-ary phase shift keying (DMPSK) constellations, was proposed in [8], which allows the use of differential detection whilst leveraging the advantages of using an increased number of receive antennas. Bit-interleaved coded modulation and iterative decoding (BICM-ID) were proposed in [9] to reduce the number of antennas up to 90% when compared to [8]. Finally, the implementation of [8] to work under a frequency selective multi-path channel was presented in [10], where the NC scheme is combined with orthogonal frequency division multiplexing (OFDM). These works showed that the NC scheme is flexible and can be integrated in various systems. Its performance superiority in scenarios with stringent conditions, as compared to the coherent scheme, makes it a good candidate for future communication systems. These papers also showed via numerical simulations that spatial correlation is detrimental to the performance of NC detection.

To further increase the performance of the NC scheme, [8] proposed to multiplex several user equipments (UEs) in the constellation domain. At the BS, a joint-symbol is received, as a result of superposing all individual symbols transmitted by each UE with their different channel effects, in the same time-frequency resource. The individual constellation adopted by each UE is crucial to produce a joint-constellation capable of unambiguously obtaining the transmitted information of these UEs. The constellation design for NC schemes combined with massive single-input multiple-output (SIMO) was performed

This work has received funding from the European Union Horizon 2020 research and innovation programme under the Marie Skłodowska-Curie ETN TeamUp5G, grant agreement No.813391, and from Spanish National Project IRENE-EARTH (PID2020-115323RB-C33) (MINECO/AEI/FEDER, UE). The work of O. A. Dobre has been supported in part by the Natural Sciences and Engineering Research Council of Canada (NSERC), through its Discovery program.

M. J. Lopez-Morales, K. Chen-Hu and A. Garcia-Armada are with Universidad Carlos III de Madrid, Spain. e-mail: ({mjlopez, kchen, agarcia}@tsc.uc3m.es). O. A. Dobre is with Memorial University, Canada. e-mail: (odobre@mun.ca).

analytically in [13], focusing on differential amplitude phase shift keying (DAPSK) and the use of uniquely factorable constellations, for the single-user case. Suboptimal constellations for the multiuser scenario based on energy detection schemes were proposed in [14]. A small set of suboptimal constellations for the multiuser case were proposed in [8] and [9], for the NC based on DMPSK namely Type A, Type B, and equal error protection (EEP), with the first one based on designing the constellation to separate the users over subquadrants, the second one based on separating the elements via power control of the users and the third one based on placing the constellation elements of each user with a certain phase shift with respect to the others. Thus, the previously designed constellations either focused on the single user case, were limited to suboptimal solutions for the multiuser case, or were applied to NC techniques not based on the DMPSK modulation, hence performing worse for the same number of antennas. Therefore, they were lacking the ability to multiplex a reasonable number of users sharing the same time-frequency resources, which is an important feature of any massive MIMO system and is also desirable when NC processing is performed.

In this paper, we aim to solve the problem of constellation design for the multiuser NC massive SIMO based on DMPSK. For this, numerical optimization problems are defined to minimize the BER and are solved offline using evolutionary computation techniques. We propose two constellation design techniques, intended to be executed offline, for which an analysis of the statistical distribution of the received joint-symbols is presented for NC massive SIMO based on DMPSK. It is shown that the distribution is different for each joint-symbol and varies depending on the individual constellations. Therefore, the model is intractable when differential encoding/decoding is chosen, making the analytical design unfeasible, and thus, forcing us to rely on numerical design techniques. The constellation design techniques can cope with different numbers of UEs and different sizes for the individual constellations, while [8] and [9] focused on a small subset. The main contributions of our paper are highlighted as follows:

1) A Gaussian-approximated optimization (GAO) approach is proposed, assuming the received joint-symbols follow a bivariate Gaussian distribution; it is based on breaking the design problem into two independent optimization problems. The former obtains the individual constellations of the UEs that best resemble a quadrature amplitude modulation (QAM) like joint-constellation and the latter obtains a bit mapping policy for each UE.
2) A Monte-Carlo based optimization (MCO) is proposed as an optimization problem based on the Monte-Carlo methods; this is able to provide the bit mapping policy and the individual constellation of all UEs with only one optimization problem. It is based on evaluating the bit error rate (BER) via Monte-Carlo simulation. It outperforms GAO and can be applied regardless of the characteristics of the propagation channel.
3) Since the optimization problems are non-convex, we propose evolutionary computation (EC) [15] to solve the optimization problems. An analysis of the complexity of the two techniques is provided, and three strategies to reduce the execution time are proposed. However, this is not critical since the GAO and the MCO are executed offline.
4) Following the proposed techniques, we provide new constellations for NC massive SIMO based on DMPSK, for several scenarios and configurations of number of users and/or constellation sizes, that are shown to outperform the state-of-the-art (SoA) via numerical simulations. We also give some insights on how to apply these constellations in realistic scenarios in real time and show via simulations that the non-coherent scheme outperforms the coherent scheme for 5G channel models with very high mobility and/or low SNR.

The remainder of the paper is organized as follows. Section II presents the system model; Section III analyzes the probability density function (PDF) of the joint constellation; Section IV develops two novel EC-based constellation design techniques; Section V analyzes the complexity of the proposed techniques and how to reduce it; Section VI presents proposals of constellations and give insights on the implementation aspects; Section VII shows numerical results of the constellations and compare the coherent and non-coherent schemes in 5G scenarios; finally, Section VIII concludes the paper.

Notation: matrices, vectors and scalar quantities are denoted by boldface uppercase, boldface lowercase, and normal letters, respectively. $[\mathbf{A}]_{m,n}$ denotes the element in the m-th row and n-th column of $\mathbf{A}$. $[\mathbf{a}]_n$ represents the n-th element of vector $\mathbf{a}$. $(\cdot)^H$, $(\cdot)^*$ and $*$ denote Hermitian, complex conjugate and convolution, respectively. $\mathbb{E}\{\cdot\}$ is the expected value. $\mathcal{CN}(0,\sigma^2)$ represents the circularly-symmetric and zero-mean complex normal distribution with variance σ^2. $f(a|b)$ is the conditional PDF of a conditioned to b. diag$(\cdot)$ indicates the diagonal matrix. $\mathfrak{R}$ and $\mathfrak{I}$ refer to the real and imaginary parts of a complex number, respectively. $Q(\cdot)$ indicates the Q-function. $x!$ is the factorial of x. $||x||_2$ denotes the Euclidean norm of x. $\angle(x)$ indicates the phase of x. $\Gamma(a,b)$ represents the Gamma function with parameters a and b.

II. System Model

We consider a BS equipped with R antennas that serves U single antenna UEs. Focusing on the UL, the UEs concurrently transmit to the BS using an NC scheme based on differential modulation. At the n-th time instant, the bits transmitted by the u-th UE are grouped in the vector $\mathbf{b}_u^n$ of size $\left(N_b^u \times 1\right)$, where N_b^u indicates the number of bits for user u, and it is mapped into a complex symbol s_u^n as

$$s_u^n = g_B(\boldsymbol{\varpi}_u, \mathbf{b}_u^n) \in \mathfrak{M}_u, \;\; \mathfrak{M}_u = \left\{c_1^u, \ldots, c_{M_u}^u\right\}, \qquad (1)$$

$$c_i^u \in \mathbb{C}, \;\; |c_i^u| = 1, \;\; c_i^u \neq c_{i'}^u \;\; \forall i \neq i',$$

where $M_u = |\mathfrak{M}_u| = 2^{N_b^u}$, $g_B(\cdot)$ is the bit mapping function, $\mathfrak{M}_u$ denotes the individual constellation set for the u-th UE (constrained to constant modulus to facilitate the use of the differential modulation), and $\boldsymbol{\varpi}_u$ of size $(M_u \times 1)$ denotes the bit mapping policy for the u-th UE which satisfies that $[\boldsymbol{\varpi}_u]_i \in \{1, \ldots, M_u\}, 1 \leq i \leq M_u, \; [\boldsymbol{\varpi}]_i \neq [\boldsymbol{\varpi}]_{i'}, \; \forall i \neq i'$. We define $\boldsymbol{\Pi} = \begin{bmatrix}\boldsymbol{\varpi}_1^T & \cdots & \boldsymbol{\varpi}_U^T\end{bmatrix}^T$ a vector of size

($\sum_{u=1}^{U} M_u \times 1$) that contains the bit mapping policies of all UEs. The complex symbols of each UE are encoded as

$$x_u^n = x_u^{n-1} s_u^n, \quad n > 0, \tag{2}$$

where x_u^n is the differentially encoded complex symbol at the n-th time instant from the u-th UE and x_u^0 is a single known reference symbol of the u-th UE. Assuming a flat-fading[1] channel, the received signal is

$$\mathbf{y}^n = \mathbf{H}^n \boldsymbol{\beta} \mathbf{x}^n + \boldsymbol{\nu}^n, \tag{3}$$

$$\mathbf{x}^n = \left[x_1^n, \cdots, x_U^n\right]^T \text{ and } \quad \boldsymbol{\beta} = \text{diag}\left(\left[\sqrt{\beta_1}, \cdots, \sqrt{\beta_U}\right]\right), \tag{4}$$

where $\boldsymbol{\nu}^n$ is the additive white Gaussian noise (AWGN) vector with each element distributed as $[\boldsymbol{\nu}^n]_r \sim \mathcal{CN}(0, \sigma_\nu^2)$, β_u denotes the ratio of the received average power of the u-th UE, with respect to user 1 ($\beta_u^{\min} = 1$, $\beta_u \geq 1$, without loss of generality), which is proportional to the composition of the large-scale channel effects and the power control of each user. A different β_u value for each user affects their performance, which is taken into account in the design of constellations. A certain $\beta_{\max}$ is considered to avoid users' performance to be excessively unequal. Moreover, $\mathbf{H}^n \in \mathbb{C}^{R \times U}$ represents the small-scale fading as a spatially uncorrelated channel matrix, where each element is distributed as $[\mathbf{H}^n]_{r,u} \sim \mathcal{CN}(0,1)$. The reference SNR is defined as

$$\rho = \frac{1}{\sigma_\nu^2} \sum_{u=1}^{U} \beta_u = \sum_{u=1}^{U} \frac{\beta_u}{\sigma_\nu^2} = \sum_{u=1}^{U} \rho_u, \tag{5}$$

where ρ_u is the SNR of user u.

The phase difference of two consecutive symbols received at each antenna is non-coherently detected as

$$\begin{aligned} z^n &= \frac{(\mathbf{y}^{n-1})^H \mathbf{y}^n}{R} = \frac{1}{R}(\mathbf{H}^{n-1}\boldsymbol{\beta}\mathbf{x}^{n-1} + \boldsymbol{\nu}^{n-1})^H (\mathbf{H}^n \boldsymbol{\beta}\mathbf{x}^n + \boldsymbol{\nu}^n) = \\ &= \frac{1}{R}(\mathbf{x}^{n-1})^H \boldsymbol{\beta} (\mathbf{H}^{n-1})^H \mathbf{H} \boldsymbol{\beta} \mathbf{x}^n + \frac{1}{R}(\mathbf{x}^{n-1})^H \boldsymbol{\beta} (\mathbf{H}^{n-1})^H \boldsymbol{\nu}^n + \\ &+ \frac{1}{R}(\boldsymbol{\nu}^{n-1})^H \mathbf{H}^n \boldsymbol{\beta} \mathbf{x}^n + \frac{1}{R}(\boldsymbol{\nu}^{n-1})^H \boldsymbol{\nu}^n. \end{aligned} \tag{6}$$

For a very large number of antennas, using the asymptotic property of massive SIMO, by making use of the Law of Large Numbers, assuming that $\mathbf{H}^{n-1} \approx \mathbf{H}^n$ and as shown in [16], we know that $\frac{1}{R}(\mathbf{H}^{n-1})^H \mathbf{H}^n \xrightarrow{R \to \infty} \mathbf{I}_U$, and thus

$$z^n \xrightarrow{R \to \infty} \varsigma^n = \sum_{u=1}^{U} \beta_u s_u^n \in \mathfrak{M}, \quad M = |\mathfrak{M}| = \prod_u M_u, \tag{7}$$

where $\mathfrak{M} = \{c_1, \ldots, c_M\}$, $c_i \in \mathbb{C}$, $c_i \neq c_{i'}$ $\forall i \neq i'$, ς^n is the joint-symbol which results from the superposition of the symbols sent by the users, and $\mathfrak{M}$ denotes the joint-constellation set. Fig. 1 shows the joint-constellation built from two particular individual constellations. We define $\mathbf{b}_{i,u}$ as a vector of size ($N_b^u \times 1$) that contains the bits for the u-th UE and the i-th joint-symbol according to the mapping $\boldsymbol{\Pi}$, and $\mathbf{b}_i = [\mathbf{b}_{i,1}^T \ \cdots \ \mathbf{b}_{i,U}^T]^T$ as a vector of size ($\sum_{u=1}^{U} N_b^u \times 1$) that contains the $\mathbf{b}_{i,u}$ of all UEs for the i-th joint-symbol.

[1]For non-flat fading channels, we can use OFDM, therefore creating multiple parallel channels that are regarded as flat-fading.

III. Interference Analysis

In this section, we first analyze the PDF of the received differentially processed signal based on DMPSK and show that it is mathematically intractable for a classical constellation design approach. For simplicity purposes, an independent-and-identically-distributed (IID) Rayleigh channel is used as it leads to the same mathematical intractability reasoning as more complex channel models. Later, to clarify that reasoning, we particularize the analysis for a set of constellations to demonstrate an inherent problem of NC differential detection that makes the individual constellations of the users and the joint-constellation non-linearly dependent.

A. Analysis of the Distribution of the Interference

The terms of (6) are shown to be independent in the Appendix of [17], and thus,

$$z^n = z_g^n + z_s^n + z_x^n = \sum_{l=1}^{3} z_{g,l}^n + z_s^n + z_x^n \tag{8}$$

where

$$z_{g,1}^n = \frac{1}{R} \sum_{r=1}^{R} \left[\boldsymbol{\nu}^{n-1}\right]_r^* [\boldsymbol{\nu}^n]_r \tag{9}$$

$$z_{g,2}^n = \sum_{u=1}^{U} \underbrace{\frac{1}{R} \sum_{r=1}^{R} \left[\boldsymbol{\nu}^{n-1}\right]_r^* [\mathbf{H}]_{r,u}}_{\tilde{z}_{g,2}^u} \sqrt{\beta_u} \, [\mathbf{x}^n]_u \,, \tag{10}$$

$$z_{g,3}^n = \sum_{u=1}^{U} \underbrace{\frac{1}{R} \sum_{r=1}^{R} [\boldsymbol{\nu}^n]_r \, [\mathbf{H}]_{r,u}^*}_{\tilde{z}_{g,3}^u} \sqrt{\beta_u} \left[\mathbf{x}^{n-1}\right]_u^* , \tag{11}$$

$$z_s^n = \sum_{u=1}^{U} \underbrace{\frac{1}{R} \sum_{r=1}^{R} \left|[\mathbf{H}]_{r,u}\right|^2}_{\tilde{z}_s^u} \beta_u s_u^n = \sum_{u=1}^{U} \tilde{z}_s^u \beta_u \exp\left(j\phi_s^{u,n}\right), \tag{12}$$

$$z_x^n = \sum_{u=1}^{U} \sum_{\substack{u'=1 \\ u \neq u'}}^{U} \frac{1}{R} \sum_{r=1}^{R} \underbrace{\sqrt{\beta_u} \, [\mathbf{H}]_{r,u}^* \sqrt{\beta_{u'}} \, [\mathbf{H}]_{r,u'}}_{\tilde{z}_x^{u,u'} = \tilde{z}_x^u \tilde{z}_x^{u'}} \left[\mathbf{x}^{n-1}\right]_u^* [\mathbf{x}^n]_{u'} \,, \tag{13}$$

where $\phi_s^{u,n} = \angle(s_u^n)$. The terms (9), (10) and (11) are noise components, (12) is the distorted (since $R < \infty$) received joint-symbol and (13) is the inter-user interference.

The distribution of the received joint symbol can be obtained using the independence of the terms in (8) and the analysis in [7]. It utilizes the properties of the product of independent complex circularly symmetric Gaussian variables [18], the properties of the modified Bessel function of the second kind and zero-th order [19], and the central limit theorem (CLT) to approximate the distribution of each term. The distribution of variables $z_{g,1}^n$, $\tilde{z}_{g,2}^u$ and $\tilde{z}_{g,3}^u$, which are defined in (9)-(11), can be asymptotically approximated for an increasing number of antennas at the BS as

$$z_{g,1}^n \sim \mathcal{CN}\left(0, \frac{\sigma_\nu^4}{R}\right), \qquad \tilde{z}_{g,2}^u, \, \tilde{z}_{g,3}^u \sim \mathcal{CN}\left(0, \frac{\sigma_\nu^2}{R}\right), \tag{14}$$

This article has been accepted for publication in IEEE Transactions on Communications. This is the author's version which has not been fully edited and content may change prior to final publication. Citation information: DOI 10.1109/TCOMM.2022.3217575

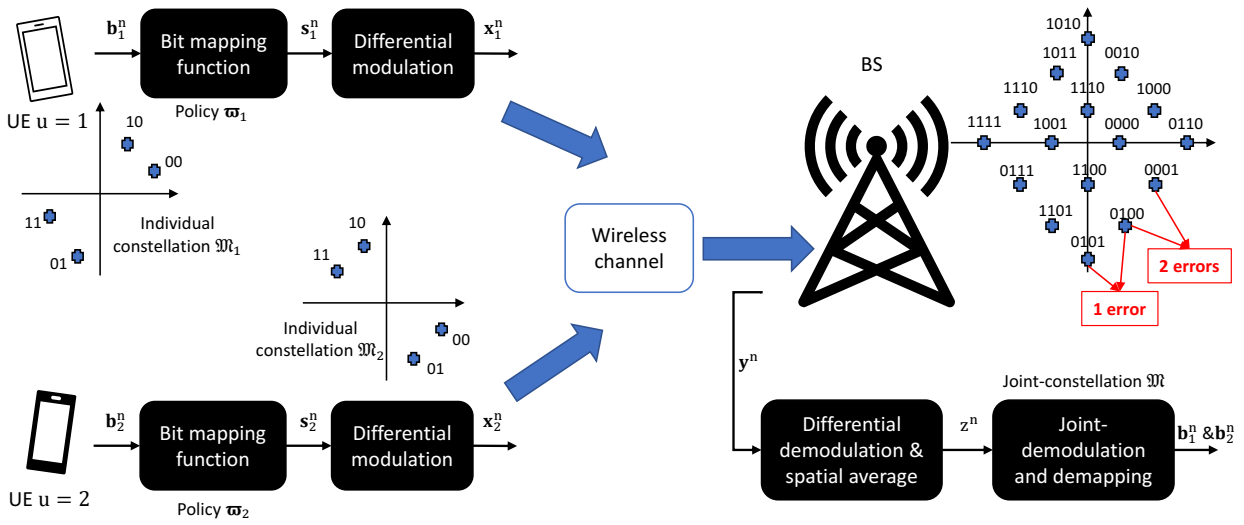

Fig. 1. Block diagram of NC scheme in UL for the particular case of $U = 2$, $\beta_1 = \beta_2 = 1$ and two particular cases of individual constellations ($\mathfrak{M}_1$ and $\mathfrak{M}_2$). These two individual constellations are properly designed by the proposed methods to produce a QAM joint-constellation ($\mathfrak{M}$).

and by using some straightforward manipulations

$$z^n_{g,2},\ z^n_{g,3} \sim \mathcal{CN}\left(0, \frac{\sigma_v^2}{R}\sum_{u=1}^{U}\beta_u\right), \tag{15}$$

since a phase rotation does not change the distribution of a bivariate Gaussian. Focusing on (12) and using [20], it can be shown that $\tilde{z}^u_s$ is a one-dimensional random variable distributed as $\tilde{z}^u_s \sim \Gamma\left(R, R^{-1}\right)$. This term only affects the amplitude of the signal, and thus, z^u_s is distributed as

$$f\left(\Re\left\{z^n_s\right\} \mid \varsigma^n\right) = \sum_{u=1}^{U}\Gamma\left(R, \frac{\beta_u}{R}\cos\left(\phi^{u,n}_s\right)\right), \tag{16}$$

$$f\left(\Im\left\{z^n_s\right\} \mid \varsigma^n\right) = \sum_{u=1}^{U}\Gamma\left(R, \frac{\beta_u}{R}\sin\left(\phi^{u,n}_s\right)\right), \tag{17}$$

where both (16) and (17) represent the summation of U independent random variables, each following a Gamma distribution with a different scale parameter (β_u and $\phi^{u,n}_s$). We can see that the distribution of this interference term, given in (12), depends on the received joint-symbol, which is the result of superimposing the symbols transmitted by all the UEs (s^n_u). Hence, the design of a robust joint-constellation against interference and noise terms is not straightforward since each joint-symbol has a different distribution.

The term (13) is a sum of $U(U-1)$ independent terms, so its conditional distribution given the differential symbols can be expressed as

$$\begin{aligned} &f\left(z^n_x \mid \phi^{u,n-1}_x, \phi^{u',n}_x,\ 1 \le u, u' \le U,\ u \ne u'\right) = \\ &= f\left(\tilde{z}^{1,2}_x\right)\exp\left(j\left(\phi^{1,n-1}_x - \phi^{2,n}_x\right)\right) * \\ &* f\left(\tilde{z}^{1,3}_x\right)\exp\left(j\left(\phi^{1,n-1}_x - \phi^{3,n}_x\right)\right) * \cdots * \\ &* \cdots * f\left(\tilde{z}^{u,u-1}_x\right)\exp\left(j\left(\phi^{u,n-1}_x - \phi^{u-1,n}_x\right)\right), \end{aligned} \tag{18}$$

where $\phi^{u,n}_x = \angle(x^n_u)$, $\tilde{z}^{u,u'}_x$, $1 \le u, u' \le U, u \ne u'$ is the product of $\tilde{z}^u_x$ and $\tilde{z}^{u'}_x$ distributed as $\mathcal{CN}(0, \beta_u)$ and $\mathcal{CN}(0, \beta_{u'})$, respectively. The analytical expression of $f\left(\tilde{z}^{u,u'}_x\right)$ can be obtained by using [21], and it is shifted by the phase difference between the differential symbols of each pair of UEs. Thus, we can see that the distribution of (13) is generated by the existence of multiple UEs, due to the fact that the off-diagonal elements of $\mathbf{H}^H\mathbf{H}$ are non-zero values. Consequently, (13) depends on the cross-product of the transmitted differential symbol by each pair of UEs (phase difference between two differential symbols), which complicates the design of the joint-constellation due to the high number of possible combinations ($\phi^{u,n-1}_x - \phi^{u',n}_x$).

Since the terms of (8) are independent, the conditional PDF of z^n given the transmitted symbols of each UE can be analytically obtained as a convolution of the PDF of each of the terms computed in (14)-(18). Assuming equiprobable joint-constellation elements, the decision of ς^n while receiving z^n can be done using (7) and maximum likelihood detection as

$$\begin{aligned} \widehat{\varsigma}^n_{ML} = \arg\max_{\varsigma^n}\{f(z^n \mid \varsigma^n, \phi^{u,n-1}_x, \phi^{u',n}_x)\} \in \mathfrak{M}, \\ 1 \le u, u' \le U, u \ne u'. \end{aligned} \tag{19}$$

From the previous analysis, it can easily be observed that the variances of the real and imaginary parts of z^n increase with increasing U. To reduce the symbol error rate (SER) and based on the previous analysis, the different elements of the joint-constellation should be placed such that the interference among them is minimized. However, the complexity of the constellation design significantly increases since the PDF differs for each joint-symbol. Moreover, even if an optimum joint-constellation is found, the individual constant modulus constellations must produce that joint-constellation and fulfill the individual requirements, described in Section II, which may not be possible. This is aggravated by the interdependent relation between the individual constellations of the users and the PDF of the received joint-constellation in the base station.

B. Effect of the Individual Constellations of the Users

In this section, the relation between the individual users' constellations, the minimum distance in the joint-constellation and the PDF of the joint-symbols are shown with some particular examples of individual and joint-constellations. For this purpose, we choose 4 different constellations of 2 users with 4 symbols per user, as shown in Fig. 2.

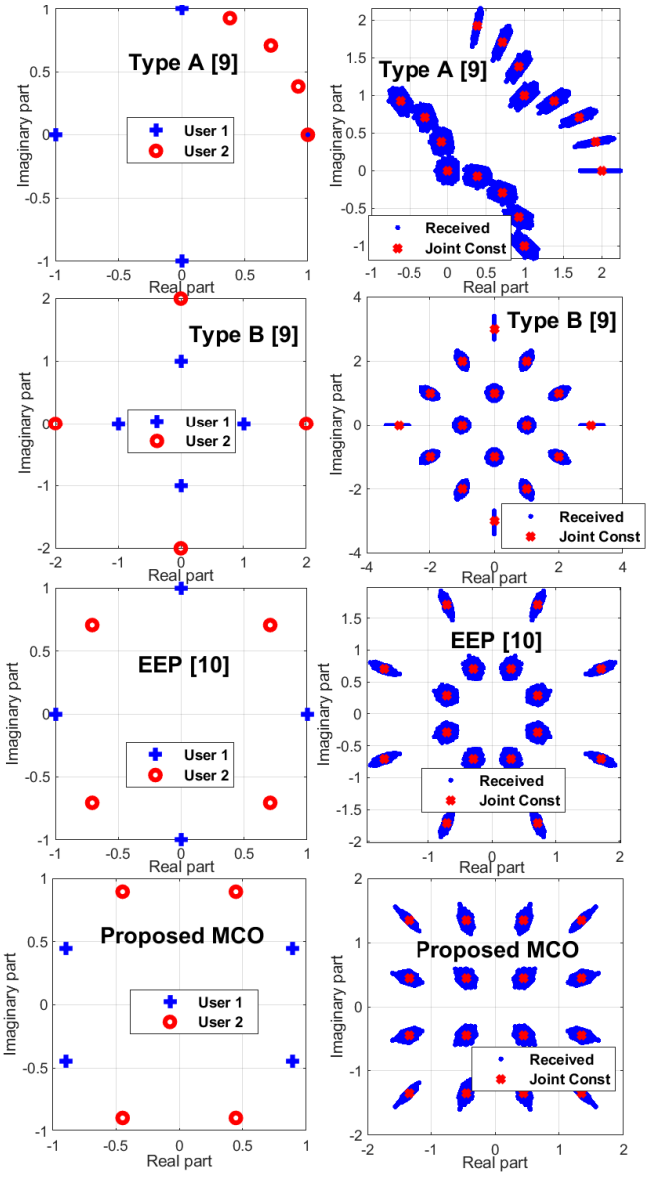

Fig. 2. Constellations for 2 users with 4 symbols per user. From top to bottom: Type A [8], Type B [8], EEP [9] and proposed MCO, left: individual constellations, right: joint-constellation. Blue dots in the right show the 2 dimensional shape of the received symbols obtained via Monte Carlo for $R = 1000$ and $\rho = \infty$.

The minimum distance between the elements in the joint-constellation must be normalized as it is done in Eq. (17) of [8], $d_{\min}^{\text{norm}} = d_{\min}/\sqrt{\sum_{u=1}^{U} \beta_u^2}$. The value of this distance for the constellations shown in Fig. 2 is: 0.39 for Type A, 0.6325 for Type B, 0.4142 for EEP and 0.6325 for the MCO. Type A reduces the distance exponentially with increasing number of users and/or constellation sizes, EEP suffers from a distance reduction in the inner circle, inherent to the constellation definition structure (making the distance even 0 in some configurations) and Type B is limited to DQPSK and the need of specific average receive powers. The normalized minimum distance (NMD) is directly related to the performance as it was shown in [8], and hence, the larger the NMD the better the performance. The NMD of the joint-constellation reduces with a greater number of users U, and/or constellation sizes M_u, thus a decrease in performance. A regular M-QAM joint-constellation maximizes the NMD, as $((M-1)/6)^{-1/2}$, so the minimum distance of any joint-constellation will fulfill $0 < d_{\min}^{\text{norm}} \leq ((M-1)/6)^{-1/2}$, with M calculated by using (7).

Furthermore, it can be observed in Fig. 2 that the distribution of the received symbols around the theoretical (obtained with $R \to \infty$) ones in the joint-constellation varies depending on the individual users' symbols. Thus, the analysis made in Eq. (17) of [8] is just valid as an approximation since it assumes that the interference of all the joint-constellation elements are bivariate Guassians, which is not the case as shown in Fig. 2. The more similarity between the phases of the individual constellation elements that compose the joint-constellation element, the larger interference power projects on its direction, while the opposite also holds. It can be observed that the interference shapes of the joint constellation elements depend on the individual constellations, and that by changing the joint-constellation shape to minimize the effect of the interference will result in the need to use different individual constellations, thus creating a different interference and resulting in a recursive problem in the design process.

IV. Proposed Constellation Designs

Traditionally, the constellation design for coherent schemes is performed for a single user, assuming that MIMO processing based on CSI can separate the streams of the UEs. The noise and interference terms are usually modelled as bivariate Gaussians, and as such, QAM constellations are preferred. Lastly, the bit mapping policy is often done using Gray coding.

However, the constellation design is more challenging for NC schemes, especially for the multiuser case, as it was demonstrated in Section III. At the same time, it is instrumental to achieve an efficient use of the time-frequency resources, allowing to multiplex several users. In Fig. 1, we outline the key points to improve the performance of the NC scheme based on differential modulation. Firstly, the joint-constellation $\mathfrak{M}$ must be robust against the interference and noise terms (see (8)-(13)). When differential modulation is used, QAM constellations are not necessarily optimum since the noise and interference terms do not follow a Gaussian distribution. Once the joint-constellation is chosen, the individual constellation for each UE ($\mathfrak{M}_u$) must be found so that when combined for all users, they create the adequate joint-constellation. However, these individual constellations may not exist, forcing us to choose an alternative joint-constellation. Finally, a bit mapping policy is required to minimize the BER.

In this section, taking into account the mathematical intractability shown in section III, we propose two approaches (GAO and MCO) to obtain the desired constellation for

each UE by numerically solving the identified non-convex, non-linear and stochastic optimization problems. Due to its potential to solve these types of problems, we choose evolutionary computation (EC) (explained in the next section) as the algorithm to solve the optimization problems defined in GAO and MCO, which are explained after the EC. To make certain that a good solution is attained, we ensure that the performance obtained by our proposed algorithm is (at the very least) better than that of the SoA or the most similar existing scenarios (given the number of users and constellation sizes of these users).

A. Evolutionary Computation (EC)

EC is a subfield of artificial intelligence [15], which is composed of global optimization techniques based on mimicking biological evolution. It has been applied to produce optimized solutions for a wide range of complex non-convex optimization problems when classical optimization techniques are not applicable, since the objective function is discontinuous, non-differentiable, stochastic, or highly non-linear. The EC complexity is characterized by the population and generation sizes (N_P and N_G, respectively); hence, N_P denotes all possible solutions to the problem evaluated to generate new descendants, and N_G is the number of times the population evolves. If N_P and N_G are properly set, very good (sometimes optimal) solutions can be found, within a certain period of time, for problems where the optimization parameters are continuous, as explained in [22] and related works. Even though EC techniques consist of an optimization search with a random component, they ensure finding practical solutions almost always to a wide range of problems in case they are properly configured. This is in contrast with machine learning techniques which easily end in local minima. To ensure the convergence of our algorithms, we checked the convergence curves for best and mean fitness (omitted in this work for space constraints) in real time and verified that the algorithm outperformed the state-of-the-art by a large margin.

From the discussion in Section III-A, we can observe that the constellation design for a multiuser NC scheme based on differential modulation turns into a mathematically intractable problem, so a numerical optimization is proposed. The optimization problems presented in (21), (23) and (24) not only are non-convex, non-linear and stochastic, but they also show a significant complexity. Given the EC benefits, we adopt the genetic algorithm [23] as a solver. It is worth noting that the approach followed in this manuscript can be extended to other non-coherent techniques such as those based on energy detection [4] or even to coherent techniques. The specific configuration of the evolutionary algorithm depends on the scenario parameters such as number of users, constellation sizes and mean received power per user, which are detailed in the next sections. For illustration purposes, the configurations in this work are shown in Table III. In the next subsections, we explain the two proposed design algorithms (GAO and MCO) that utilize the GA as a solver of the numerical optimization problems.

B. Gaussian-Approximated Optimization (GAO)

As a first approximation to simplify the design process (valid for low SNR and R values since the noise term (z_g^n) dominates), the conditional distribution of z^n given the transmitted symbols of each UE provided in (19) is approximated as a bivariate Gaussian distribution for all the joint-symbols in the joint-constellation ($\mathfrak{M}$). Thus, the classical regular QAM constellation [24] can be straightforwardly set as the joint-constellation. The problem relies on finding the individual constellations that resemble, as reliably as possible, a regular QAM joint constellation.

To ease the notation, let us define the constellation vectors for the objective normalized QAM joint-constellation, that is, the joint constellation that we would like to approach as close as possible, and the actual individual constellation of the u-th UE, respectively, as

$$\mathbf{c} = \begin{bmatrix} c_1 & \cdots & c_M \end{bmatrix}^T, \quad \tilde{\mathbf{c}}_u = \begin{bmatrix} [\tilde{\mathbf{c}}_u]_1 & \cdots & [\tilde{\mathbf{c}}_u]_{M_u} \end{bmatrix}^T, \tag{20}$$

where $[\tilde{\mathbf{c}}]_i$ is the obtained joint-constellation and is defined as

$$[\tilde{\mathbf{c}}]_i = \sum_{u=1}^{U} \beta_u \, [\tilde{\mathbf{c}}_u]_{i_u}, \quad 1 \le i \le M, \quad \left|[\tilde{\mathbf{c}}_u]_{i_u}\right|^2 = 1,$$
$$0 \le \angle\left([\tilde{\mathbf{c}}_u]_{i_u}\right) < 2\pi, \quad u = 1, \cdots, U, \quad i_u = 1, \cdots, M_u.$$

The individual constellations must be found for each UE $\tilde{\mathbf{c}}_u$ such that, when combined with their corresponding β_u, they resemble the objective QAM joint-constellation as accurately as possible. This is achieved by solving the following problem

$$\begin{aligned} \min_{\tilde{\mathbf{c}}_u, \boldsymbol{\beta}} \quad & \alpha_1 \left\| \frac{\mathbf{c}}{||\mathbf{c}||_2} - \frac{\tilde{\mathbf{c}}}{||\tilde{\mathbf{c}}||_2} \right\|_2 + \alpha_2 \sum_{u=1}^{U} \beta_u, \\ \text{s.t.} \quad & 1 \le \beta_u \le \beta_{\max}, \quad \alpha_1 + \alpha_2 = 1. \end{aligned} \tag{21}$$

The vectors $\tilde{\mathbf{c}}$ and $\mathbf{c}$ are normalized in (21) to properly compare them, $\beta_{\max}$ is the maximum allowed ratio of the effective received power between users, and the terms α_1 and α_2 are added to allow different ways to constrain the values of β_u, $\forall u$. When $\alpha_1 << \alpha_2$, the optimization problem forces the same unitary power to all UEs ($\beta_u = 1$, $\forall u$). Otherwise, when $\alpha_1 >> \alpha_2$, it does not constrain β_u values. The optimization problem is non-convex and NP-hard, so we have to exploit numerical methods based on EC to solve this problem. More details are provided in Section IV-A.

After the individual constellations for each UE ($\tilde{\mathbf{c}}_u$, $\forall u$) and the received power coefficients (β_u, $\forall u$) are found as a solution to (21), an adequate bit mapping policy for each UE is required to guarantee a sufficiently low BER. To find this bit mapping policy, since the decision is made over the joint-symbols ($\mathbf{c}$) and since we assumed a bivariate Gaussian distribution for all joint symbols, we define an approximated BER (P_b) based on the use of the SER upper bound [25] for a certain bit mapping policy and joint-constellation

$$P_b\left(\boldsymbol{\Pi}, \mathbf{c}\right) = \sum_{i=1}^{M} \sum_{\substack{i'=1 \\ i \neq i'}}^{M} \underbrace{Q\left(\left\|[\mathbf{c}]_i - [\mathbf{c}]_{i'}\right\|_2\right)}_{p_j\left([\mathbf{c}]_i, [\mathbf{c}]_{i'}\right)} \underbrace{\frac{||\mathbf{b}_i - \mathbf{b}_{i'}||_1}{M \log_2 M}}_{\hat{P}_b\left(\boldsymbol{\Pi}, [\mathbf{c}]_i, [\mathbf{c}]_{i'}\right)} \tag{22}$$

Algorithm 1 Constellation design based on GAO

procedure GAO(M, U, α_1, α_2)
  $\mathbf{c} \leftarrow M$-QAM ▷ *Constrain the joint-constellation*
  $\tilde{\mathbf{c}}_u \leftarrow$ SearchInd($\mathbf{c}$, U, α_1, α_2) ▷ *Individual constellation*
  $\mathbf{\Pi} \leftarrow$ SearchPolicy($\tilde{\mathbf{c}}_u$, $\mathbf{c}$) ▷ *Bit mapping*
end procedure

where $p_j\left([\mathbf{c}]_i, [\mathbf{c}]_{i'}\right)$ is the joint-symbol error rate produced by the decision of $[\mathbf{c}]_{i'}$ when $[\mathbf{c}]_i$ is transmitted and $\hat{P}_b\left(\mathbf{\Pi}, [\mathbf{c}]_i, [\mathbf{c}]_{i'}\right)$ is the BER produced by the miss-decision of the joint-symbol (as the errors shown in Fig. 1). In this problem, $\mathbf{b}_i = g_B^{-1}(\mathbf{\Pi}, [\mathbf{c}]_i)$ is obtained with the inverse of the bit mapping function $g_B^{-1}(\bullet)$ which inputs the joint symbol $[\mathbf{c}]_i$ and the bit mapping policy applied at the UEs $\boldsymbol{\varpi}_u$.

Hence, the optimization problem for obtaining the optimum bit mapping policy for each UE can be described as

$$\begin{aligned} \min_{\mathbf{\Pi}} \quad & P_b\left(\mathbf{\Pi}, \mathbf{c}\right), \\ \text{s.t.} \quad & \boldsymbol{\varpi}_u \in \mathfrak{B}_u, \quad B_u = |\mathfrak{B}_u| = M_u!, \\ & [\boldsymbol{\varpi}_u]_{i_u} \neq [\boldsymbol{\varpi}_u]_{i'_u}, \quad i_u \neq i'_u, \quad 1 \leq i_u, i'_u \leq M_u, \end{aligned} \tag{23}$$

where $\mathfrak{B}_u$ is a set of bit mapping policies for the u-th UE that contains all the possible permutations of policies. The restriction $[\boldsymbol{\varpi}_u]_{i_u} \neq [\boldsymbol{\varpi}_u]_{i'_u}$ indicates that different symbols of the individual constellation of UE u cannot be mapped to the same bits. This is a finite integer optimization problem which can be solved by exploiting an exhaustive search. Nevertheless, we propose to use numerical methods based on EC when the complexity is too high, as shown in Section V.

Algorithm 1 provides a summary of the GAO. Firstly, M-QAM is chosen for the joint-constellation. Then, the individual constellations fulfilling (21) are obtained. Finally, the bit mapping policy for all UEs is obtained with (23).

C. Monte-Carlo based Optimization (MCO)

The complex circularly-symmetric Gaussian appr employed by GAO is much faster but not accurate e several realistic scenarios, and thus, it provides a s solution. Nevertheless, this solution is still useful as ization to the MCO, as will be seen in Sec. V. In the joint-constellation shape and bit mapping policy in two separate steps, which limits the GAO pos explore a more diverse set of solutions. We propose MCO, where no assumptions on the joint-constellat are considered and the bit-mapping policy is co with the joint-constellation shape. It is based on th Carlo method to numerically evaluate the perfor terms of BER of the candidates at each iteration. T optimization problem is expressed as

$$\begin{aligned} \min_{\tilde{\mathbf{c}}_u, \boldsymbol{\beta}} \quad & \alpha_1 \sum_{u=1}^{U} [\boldsymbol{\epsilon}]_u + \alpha_2 \sum_{u=1}^{U} \beta_u, \\ & \boldsymbol{\epsilon} = g_M\left(\sigma_v^2, R, \mathbf{\Pi}, \boldsymbol{\beta}, \hat{\mathbf{c}}, N_s, N_r\right) \\ \text{s.t.} \quad & \left|[\tilde{\mathbf{c}}_u]_{i_u}\right|^2 = 1, \quad 0 \leq \angle\left([\tilde{\mathbf{c}}_u]_{i_u}\right) < 2\pi, \\ & u = 1, \cdots, U; \; i_u = 1, \cdots, M_u; \; 1 \leq \beta_u \leq \beta_{\max} \\ & [\hat{\mathbf{c}}] = [\tilde{\mathbf{c}}_1, \cdots, \tilde{\mathbf{c}}_U]^T, \quad \alpha_1 + \alpha_2 = 1, \quad \boldsymbol{\varpi}_u \in \end{aligned}$$

Algorithm 2 Constellation design based on MCO

procedure MCO (M_u,N_P,N_G,σ_v^2,R,$\mathbf{\Pi}$,N_s,N_r,α_1,α_2)
  $[\mathbf{c}_u^{\text{ini}}, \beta_u^{\text{ini}}] \leftarrow$ Init(M_u, U) ▷ *Init.*
  $[\mathbf{c}_u^{\text{iter}}, \beta_u^{\text{iter}}] \leftarrow$ OptCtrl($\mathbf{c}_u^{\text{ini}}$,$\beta_u^{\text{ini}}$,$N_P$,$N_G$) ▷ *Control Init.*
  while stop==false **do**
    $\boldsymbol{\epsilon} \leftarrow$ MonteCarlo($\mathbf{c}_u^{\text{it}}$, β_u^{it}, σ_v^2, R, $\mathbf{\Pi}$, N_s, N_r)
    $f_{\text{obj}} \leftarrow$ Evaluation($\boldsymbol{\epsilon}$, β_u^{it}, α_1, α_2) ▷ *Evaluate*
    $[\mathbf{c}_u^{\text{it}}, \beta_u^{\text{it}}, \text{stop}] \leftarrow$ OptCtrl($\mathbf{c}_u^{\text{it}}$, β_u^{it}, N_P, N_G, f_{obj}) ▷ *Control*
  end while
  output: $\beta_u^{\text{end}} \leftarrow \beta_u^{\text{it}}$, $f_{\text{obj}}^{\text{end}} \leftarrow f_{\text{obj}}^{\text{it}}$, $\mathbf{c}_u^{\text{end}} \leftarrow \mathbf{c}_u^{\text{it}}$
end procedure

where $\boldsymbol{\epsilon}$ is a vector of size $(U \times 1)$ that contains the BER of each UE and $g_M(\cdot)$ denotes a function to obtain this BER for a particular set of system parameters. Similar to (21), this optimization problem is non-convex and NP-hard. Hence, we propose to solve it by using numerical methods based on EC detailed in Section IV-A.

Fig. 3 provides a block diagram of the implementation of MCO, and Algorithm 2 shows its pseudocode. The Monte-Carlo block performs a link-level simulation as described in Section II. The scenario conditions of the optimization problem are R and σ_v^2, and the Monte Carlo simulation performs N_r realizations of the channel and noise, without any constraint on their characteristics. Given the scenario conditions, the chosen individual constellations ($\tilde{\mathbf{c}}_u$), the ratio of average received power per user (β_u) and the bit mapping policies ($\mathbf{\Pi}$) of all UEs at each iteration, the Monte-Carlo block obtains the BER performance of all the UEs ($\boldsymbol{\epsilon}$ of size $(U \times 1)$). To attain an accurate enough BER, we can configure the number of symbols transmitted by each UE (N_s) at each iteration and the number of iterations (N_r). The optimization

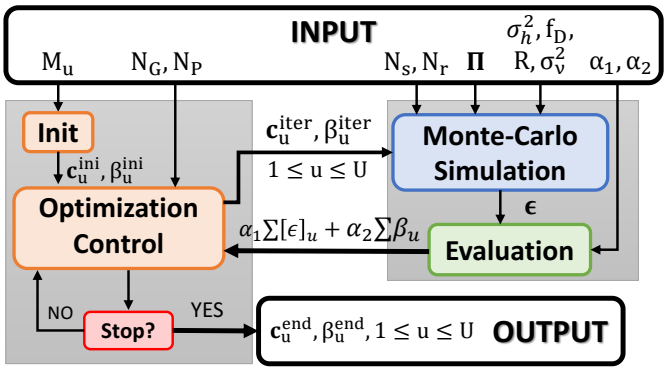

Fig. 3. Block diagram of MCO.

V. Complexity Analysis and Strategies for its Reduction

In this section, we analyze the complexity of the proposed design techniques and then, we propose strategies to reduce their complexity without losing performance.

A. Complexity Analysis

The EC complexity depends on the population size (N_P) and number of generations (N_G) [26]. They must be selected to facilitate a sufficient search of the possible results to the optimization problem. The values for N_P and N_G should be proportional to the dimensionality of the problem ($N_D = \sum M_u$), which corresponds to the number of variables to optimize ($N_D \propto N_P N_G$), to ensure an adequate solution is found. Nevertheless, they are typically obtained with some trial, error and observation of the convergence [27], [28].

To provide insight into the complexity, we look at the dimensionality of the problem. Furthermore, for each population element, we account for the number of required complex products ($N_\times$) and sums (N_+) [29]. Table I summarizes the complexity comparison for GAO and MCO.

The first optimization of GAO (21) comprises the matching between the normalized target QAM constellation $\mathbf{c}$ and the obtained joint-constellation $\tilde{\mathbf{c}}$. The dimensionality of the problem depends on M_u and U. At each iteration, the mean squared error (MSE) between the points of the target QAM and the obtained one is calculated. The number of products and sums is conditioned by the MSE computation.

The second optimization problem of GAO (23) is an integer optimization problem that can be solved by an exhaustive search, since the possible amount of combinations is finite. According to (23), the number of possible bit mapping policies depends on the constellation sizes of the users. Each user can map a different set of bits for each symbol, without repetition. Therefore, considering that user u has a constellation size M_u, the first symbol can be mapped to M_u different bit mapping sets $\{1, 2, \cdots, M_u\}$. Once the first symbol is mapped to one bit mapping policy, the second symbol can be mapped to $M_u - 1$ different bit mapping policies. We repeat until symbol M_u, so user u has a total of $M_u \times (M_u - 1) \times \cdots \times 1 = M_u!$ bit mapping policies. Considering that the users' bit mapping policies are independent, the amount of possible bit mapping policies is $N_M = \prod_{u=1}^{U} M_u! > N_P N_G$. Even though the exhaustive search is feasible, we propose the use of EC for solving this optimization problem to increase the efficiency when N_M is very large. In Section VI, we provide a numerical comparison to verify this point. The number of operations required (complex products and sums) at each iteration is determined by the computation of (22).

Finally, the dimensionality of MCO is the same as that of the first step of GAO. However, the complexity at each iteration is much higher for MCO due to the Monte-Carlo simulations. The number of operations is due to the simulation of the differential encoding/decoding, channel propagation, spatial averaging, joint-symbol decision and BER computation. Additionally, these operations are repeated $N_s \times N_r$ times to obtain an accurate enough BER estimation.

B. Strategies for Complexity Reduction

First, we note that the complexity of both steps of GAO is low enough to make the computation time negligible for today's computational capabilities. On the other hand, the MCO complexity is much higher, since a Monte-Carlo simulation is executed for each member of the population in each generation. Typically, N_G and N_P should be large enough to produce a high number of diverse potential solution candidates to be evaluated [26], to obtain a reliable-enough global minimum. However, this method (denoted as S1) excessively increases the execution time for the proposed MCO. Accordingly, we propose two strategies (S2 and S3) to reduce the complexity.

S2 is based on a hierarchical search to reduce N_P and N_G without sacrificing the performance, being built on two phases: exploration and refinement. In the exploration phase, the evolutionary algorithm is run with a very small number of N_G, N_P, and a small number of N_r and N_s to reduce the execution time as much as possible. Hence, a better than random but still low-accuracy solution is found. This solution initializes a new run of the evolutionary algorithm in which N_s and N_r are increased, and then a more accurate solution is obtained. Both phases can be repeated several times, increasing N_P and N_G in each cycle, until a convergence criterion is met, always ensuring the summation of the product $N_P N_G N_s N_r$ for all iterations is lower than that of S1. As we will show in Section VI, the complexity is reduced to about one third of the S1, without losing on the performance of the obtained solutions.

Additionally, the solution obtained for GAO can be used as an input for MCO with reduced N_G and N_P. We first find a suboptimal but better than the SoA solution with GAO, and then refine it with MCO. This strategy is referred to as S3. The complexity is reduced to about one fourth compared to the S1, without losing performance, as shown in Section VI.

A last strategy makes use of the solution obtained from MCO for a particular scenario (fixed number of antennas, particular propagation channel and SNR). To explore other similar scenarios, we propose that the solution is employed as the initial point for the optimization problem in the new scenario, and we denote this strategy as S4. As we will show in Section VI, the complexity is reduced about some tens with respect to the S1, without losing performance.

VI. Proposed Constellations and Implementation Aspects

In this section, we first propose a set of constellations, obtained with the proposed design techniques, for the multiuser scenario of the UL of NC massive SIMO. Second, we give insights on how to implement them in real scenarios.

A. Proposed Constellations

We provide a set of constellations in Table II, which have been obtained with the strategy S3 of Section V with the parameterization in Table III and setting a random initial population. While each constellation has been determined for a certain R and ρ, it can be used for any values in a realistic range. These constellations outperform the SoA, as shown in Section VI, and can be used to propose constellations for new scenarios with different users and constellation sizes (even among users).

To read the table, please note we provide for each scenario U vectors of the form $\Phi = [\Phi_1^u \Phi_2^u \cdots \Phi_{M_u}^u]$, where $\Phi_{m_u}^u$ is

TABLE I
COMPLEXITY COMPARISON FOR GAO AND MCO.

Technique	N_D	$N_\times$ per iteration	N_+ per iteration
GAO - Individual constellation	$U + \sum_{u=1}^{U} M_u$	$\prod_{u=1}^{U} M_u$	$\prod_{u=1}^{U} M_u$
GAO - Bit mapping policy	$\sum_{u=1}^{U} M_u$	$\left(\prod_{u=1}^{U} M_u\right)^2$	$\left(\prod_{u=1}^{U} M_u\right)^2$
MCO (without complexity reduction)	$U + \sum_{u=1}^{U} M_u$	$N_s N_r \left(R(U+1) + 2\prod_{u=1}^{U} M_u\right)$	$N_s N_r \left(R(U+2) + 3\prod_{u=1}^{U} M_u\right)$

the phase in radians for the constellation element m_u of user u ($1 \leq m_u \leq M_u$, $1 \leq u \leq U$, where M_u is the constellation size of user u). A specific constellation element m_u of user u can be found as $s^u_{m_u} = \exp j\Phi^u_{m_u}$. The mapping of element m_u is obtained with a decimal to binary conversion of $m_u - 1$. An example of a constellation for 2 users with quadrature phase-shift keying (QPSK) ($\mathbf{M}$ = [4 4], $\boldsymbol{\beta}$ = [1 1]) is shown in Fig. 4 and another one for 3 users with QPSK ($\mathbf{M}$ = [4 4 4], $\boldsymbol{\beta}$ = [1 1 1]) is depicted in Fig. 6.

B. Applicability in Real Scenarios

We obtained constellations by means of an offline optimization using different scenario parameters (R, ρ_u, v, etc.). The complexity of the online stage is not affected in any case by the complexity of the offline design technique, and only the constellations look-up table is different from the previous solutions in the SoA. These constellations minimize the average BER of the users for the scenario parameters for which they have been designed. Nevertheless, the proposed constellations work well for any operative values of ρ and R.

If a better performance is desired at the expense of increasing the complexity, we may obtain constellations optimized for different R and ρ values (results are more sensitive to R than to ρ, as shown in Section VII), for the different combinations of users and constellation sizes. In this case, the proposed set of solutions would be much larger. It is worth noting that each scenario will have a fixed R, so in practice the constellations should be designed for that R and for a few ρ values.

Given the improved constellations and β_u values for a certain scenario, the scheduler at the BS may perform a user grouping, power control strategy (considering the ρ_u of the users) and modulation and coding scheme (MCS) assignment, similarly to what is done, for example, in non-orthogonal multiple access systems [30]. Based on this strategy, it would be decided which users should be multiplexed with which MCS and powers to share the same time-frequency resources, with the goal of optimizing some non-coherent multiuser massive SIMO network parameter. The user grouping and power allocation can take advantage of the different path-loss suffered by each user to help minimize the power consumption of the users. It is worth noting that a user re-grouping would be performed by the BS only when the large-scale effects vary significantly (which happens slowly). This can be triggered by two factors: some users appear or disappear from the network or the power usage required by at least one user exceeds a predefined threshold. A detailed investigation of the user grouping, power control and MCS assignment is part of a future work.

VII. NUMERICAL RESULTS FOR PERFORMANCE AND COMPLEXITY

In this section, we first present the performance of the most representative constellations, utilizing both an IID Rayleigh channel and a geometric realistic channel that undergoes both spatial and time correlation. Second, we show numerical results for the time complexity of the EC algorithm and validate the theoretical complexity analysis. Last, we provide results that justify the use of NC over coherent massive MIMO for channels with very high mobility and/or low SNR.

A. Performance Evaluation

First, the case of 2 users with QPSK is shown since it has been used in the SoA as a baseline case. It is important to demonstrate the capabilities of our design technique and the proposed solution with respect to the previous work. Second, the case of 3 users with QPSK, 2 users with 8PSK and 4 and 5 users with BPSK are shown since the SoA solutions for these scenarios proved to be very limited in terms of performance. Thus, we show that our proposed solution can greatly overcome the SoA limitations. Last, the case of 3 users with different constellation sizes is shown to illustrate that we overcome another limitation of the SoA, namely that the previous works could not propose any set of constellations with different sizes for an arbitrary number of users (e.g. $U = 3$ was not possible for several constellation sizes), while our solution can. The configuration of the evolutionary algorithm for each scenario is calculated following Table III, by setting U and M_u accordingly. We show the individual and joint constellations and the average BER of the uncoded constellations. We compare our solutions with the constellation designs in [17]. To ease the understanding of the results, the individual elements in the constellations are tagged by a number i, which corresponds to the sub-index of the complex symbols (c_i and c^u_i), described in (20). Each i indicates a bit mapping that results from the decimal to binary conversion of $i - 1$.

1) Scenario with $U = 2$ and $M_u = 4$ $\forall u$: In this scenario, there are two UEs, where each UE has a constellation of size $M_u = 4$. Moreover, in this subsection, the MCO results are obtained by setting $R = 100$ and SNR = 0 dB. The solutions obtained here are superior to the ones of Type A in [8], which is worse than Type B, so we restrict the comparison to the latter due to space limitation. When $\alpha_1 >> \alpha_2$, both GAO and MCO obtain the same solution as the constellation Type B given in [8] ($\beta_1 = 1$ and $\beta_2 = 2$), where each individual constellation corresponds to a 4-QAM and the joint-constellation corresponds to a 16-QAM. When $\alpha_1 << \alpha_2$, the solution for both GAO and MCO is $\beta_1 = \beta_2 = 1$. In Fig.

TABLE II
PROPOSED CONSTELLATIONS (PHASES IN RADIANS) FOR DIFFERENT U, M_u AND β_u. COLUMN $\mathbf{\Phi}$, HAS U VECTORS WITH M_u ELEMENTS EACH.

U	**M**	β_u	$\mathbf{\Phi}$				
2	2 2	1 1	0 3.14	1.57 4.71			
	2 4	1 1	5.87 2.71	1.89 0.87 4.31 5.53			
	2 4	1.3 1	3.69 0.41	1.53 4.63 2.88 5.98			
	2 4	1 1.95	2.3 5.84	2.49 0.97 4.49 5.61			
	2 8	1 1	5.87 4.37	3.53 0.82 4.76 2.14 1.49 0.2 5.67 5.20			
	2 8	1 1.5	3.11 0.58	0.44 3.8 3.06 4.6 1.07 1.87 6.14 5.16			
	2 8	1 1.8	3 0.11	2.8 0.92 4.41 1.58 5 3.35 5.9 0.16			
	2 16	1 1	1.08 4.42	2.55 0.1 0.9 3.6 1.91 4.94 1.22 5.56 2.79 0.47 3.01 3.32 2.17 5.21 1.53 5.95			
	4 4	1 1	0.98 4.11 1.88 5.03	0.33 5.68 2.65 3.51			
	4 4	1 2	0 3.14 1.57 4.71	0 3.14 1.57 4.71			
	4 8	1 1	2 1.08 4.64 3.82	3.4 2.91 1.69 2.01 5.41 2.58 0.2 5.99			
	4 8	2 1	1.94 0.23 3.47 5.03	4 3.26 4.73 5.27 1.75 2.64 0.29 6.07			
	4 16	1 1	3.85 3.23 0.22 0.87	1.53 1.33 1.88 1.15 2.85 5.61 5.21 5.42 2.28 0.15 2.14 4.28 2.51 6 4.95			
	4 16	1 1.4	2.52 4.56 5.5 1.48	0.5 6.2 3.46 3.77 1.5 0.7 3.3 0.85 5.6 4.43 3.06 0.27 1.3 5.92 4.14 2.5			
	4 16	2 1	3.05 1.5 4.64 6.05	1.04 1.37 0.7 1.08 6.07 5.8 0.18 6.06 2.52 1.9 3.05 3.6 5.04 5.44 4.36 4			
	8 8	1 1	1 0.6 3.65 3.24 6 0.2 4.17 2.92	4.93 5.3 4.46 5.74 2.21 1.72 2.57 1.29			
	8 8	1.12 1	5.5 5.75 5.2 6 3.2 2.36 1.8 2.7	1 4.55 0.68 1.5 0 5.06 4.08 3.57			
3	2 2 2	1 1 1	3.39 0.24	4.9 0.35	1.77 4.99		
	2 2 4	1 1 1	6.05 2.67	1.35 4.54	2.46 1.89 3.16 1.32		
	2 2 4	1.8 1.8 1	0.12 2.87	1.58 4.44	3.91 5.64 2.31 0.8		
	2 2 4	1 1.2 2.6	3.54 0.74	4.3 2.37	4.21 2.44 0.96 5.73		
	2 2 8	1 1 1	3.99 2.73	0.84 4.17	1.61 5.53 2.06 3.14 4.96 6 0.21 2.55		
	2 2 8	1 1.2 3.3	0.31 2.7	1.23 4.35	0.9 2.57 3.68 5.36 0.53 2.22 4.14 5.75		
	2 2 8	1.4 1.4 1	3.42 0.4	1.68 4.73	3.81 6.07 4.68 5.34 0.76 3.01 1.38 2.1		
	2 4 4	1 1 1	1.5 4.38	1.7 6.24 4.85 3.38	3.06 6.08 2.57 5.48		
	2 4 4	1.6 1.5 1	3.06 6.08	1.38 0.75 3.9 4.5	4.41 2.62 5.75 1.55		
	2 4 4	1 1 2.7	4.44 1.39	6.28 1.82 5 3.14	4.82 0.44 3.37 1.63		
	2 4 8	1 1 1	2.61 6.24	4.65 6.1 1.76 1.22	0.45 4.06 0.82 3.74 0.09 3.17 1.15 3.49		
	2 4 8	1.6 1.5 1	4.29 1.63	0.4 5.45 2.4 3.2	0.37 0.8 0.05 5.96 1.56 1.17 3.46 2.88		
	4 4 4	1 1 1	3.01 1.14 6.05 4.45	3.64 3.2 1.68 5.55	5.03 0.99 1.88 4.12		
	4 4 4	1 2.53 1	3.61 5.82 2.68 0.46	2.36 0.79 3.93 5.5	5.18 1.11 4.25 2.03		
	4 4 4	1 2 4	0 1.57 3.14 4.71	0 1.57 3.14 4.71	0 1.57 3.14 4.71		
4	2 2 2 2	1 1 1 1	5.06 3.93	5.9 0.69	1.72 4.78	0.13 3.24	
	2 2 2 2	2.1 1 2.1 1	3.87 0.55	5.38 2.2	5.29 2.32	3.85 0.6	
	2 2 2 4	1 1 1 1	5.84 2.54	0.87 4.51	4.61 2.5	3.4 1.88 4.19 0.44	
	2 2 2 4	2.4 1.4 2.4 1	2.85 5.97	3.63 0.58	4.75 1.32	6.01 4.77 1.62 3	
	2 2 2 8	1 1 1 1	5.89 1.01	2.96 5.58	4.17 1.14	4.95 5.3 0.3 0.64 1.7 3.5 2 3.95	
	2 2 4 4	1 1 1 1	0.91 1.33	3.96 4.4	3.15 0.06 2.63 5.89	5.57 2.4 0.42 3.87	
	2 2 4 4	3.3 3.1 1 2.3	4.23 1.21	2.49 5.78	5.15 3.42 0.28 1.9	1.78 0.38 5.01 3.46	
5	2 2 2 2 2	1 1 1 1 1	5.1 2.19	2.43 4.2	0.49 3.76	3.32 0.05	1.37 4.58
	2 2 2 2 2	1 1.1 1.6 3.4 2	0.58 4.53	4.65 2.55	3.65 0.33	3.3 6.26	1.9 5.2

4, we show the individual constellations (top) for the case of $\beta_1 = \beta_2 = 1$, and the resulting joint-constellations (bottom), for the EEP [9], GAO and MCO schemes (from left to right). For GAO and MCO, the constellation is the same and it is a 16-QAM (rotated for the MCO). For EEP, the joint-symbols placed at the inner circle have a very small distance to each other, which degrades the performance.

In Fig. 5, we plot the average BER of both UEs for the EEP, GAO and MCO, where GAO and MCO significantly outperform EEP. The bit mapping policy is key to the performance of the system, as shown by intentionally replacing the bit mapping policy by a bad one denoted "bad map" in Fig. 5, where we can see the performance degradation. Moreover, by inspecting Fig. 4, we can understand that GAO and MCO reduce the BER with respect to EEP by increasing the distance among joint symbols and reducing the pairwise bit errors.

2) Scenario with $U = 3$ and $M_u = 4$ $\forall u$: In this scenario, we increase the number of UEs to three, and each UE has an individual constellation of size $M_u = 4$. The results provided by the MCO are obtained for $R = 400$ and SNR = 3 dB. In Fig. 6, we show the individual constellations (top) for both UEs and the joint-constellation (bottom) for EEP, GAO and MCO (from left to right), when $\beta_u = 1$, $\forall u$. EEP cannot be used

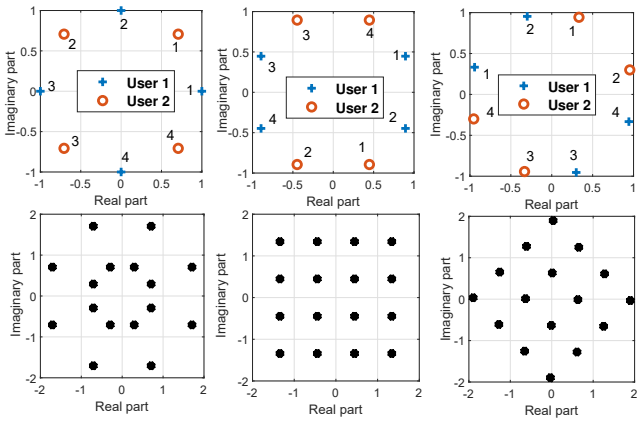

Fig. 4. Constellations for 2 users with 4 symbols per user with $\beta_u = 1$. From left to right: EEP, GAO and MCO. Top: individual users constellations, bottom: joint-constellation.

for three UEs as different combinations of individual symbols generate the same joint-symbols, since 11 joint-symbols out of 64 are equal in the complex-plane, thus creating an error floor of $11/64 \approx 0.172$, something avoided by GAO and MCO. In Fig. 7, we provide the average BER vs. ρ; our proposed

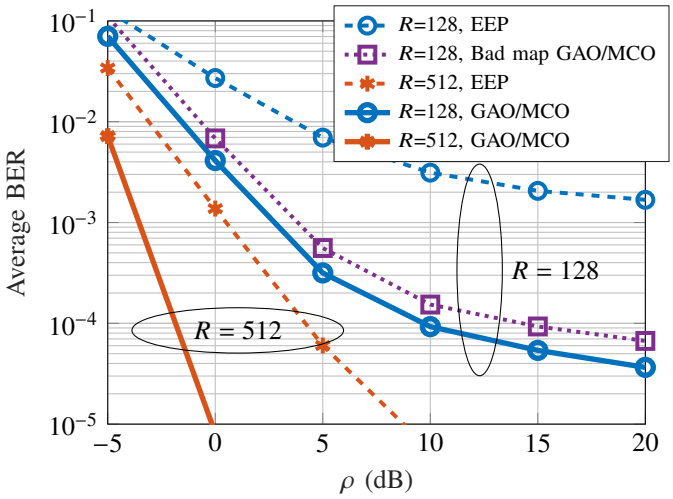

Fig. 5. BER vs. ρ for 2 users and 4 symbols per user with $\beta_u = 1$.

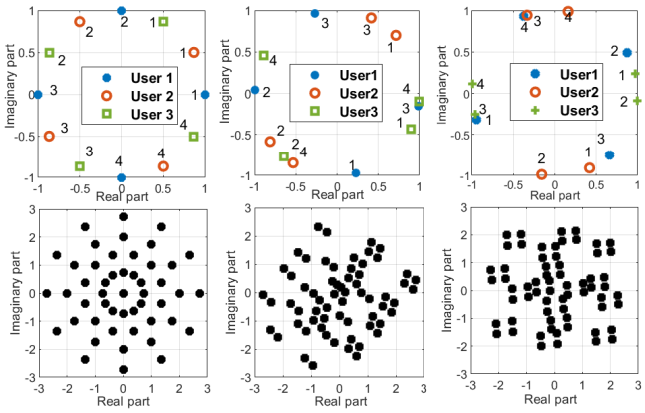

Fig. 6. Constellations for 3 users with 4 symbols per user with $\beta_u = 1$. From left to right: EEP, GAO and MCO. Top: individual users constellations, bottom: joint-constellation.

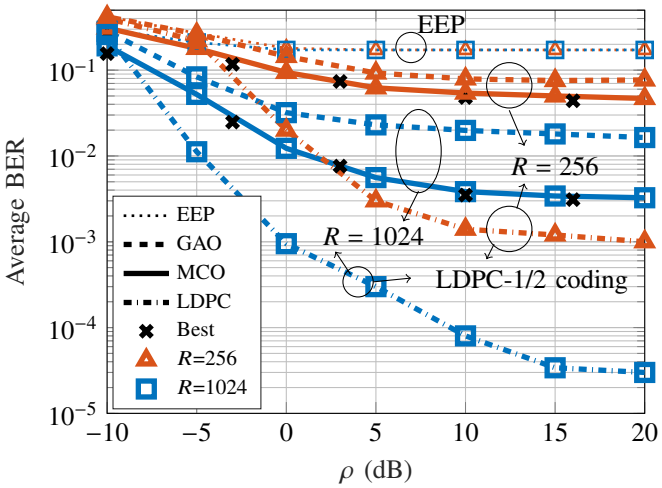

Fig. 7. BER vs. ρ for 3 users and 4 symbols per user with $\beta_u = 1$, for $R = 256$ and $R = 1024$. Black crosses show the best performance with MCO optimized for those values. The performance with LPDC-1/2 coding is shown.

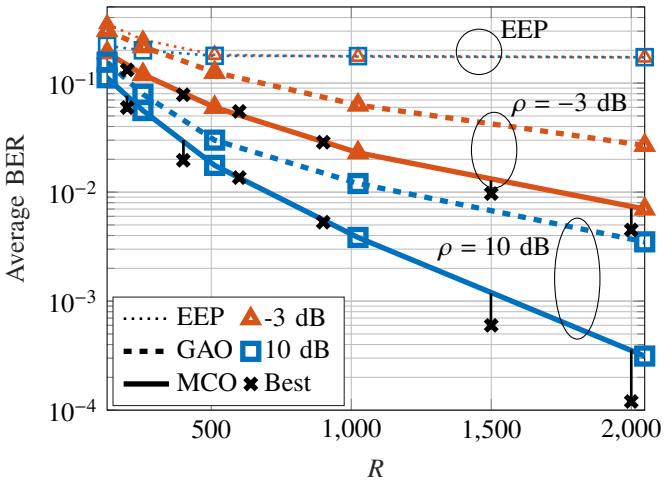

Fig. 8. BER vs. R for 3 users and 4 symbols per user with $\beta_u = 1$, for SNR=-3 dB and SNR=10 dB, for the EEP, the GAO and the MCO. Black crosses show the best performance with MCO optimized for those values.

schemes significantly outperform EEP, and MCO performs the best. In fact, these results confirm the mentioned error floor of EEP. Additionally, we show with black crosses the performance when MCO is trained for ρ values different from the one used for the optimization, leaving R unchanged. It can be seen that the effect of ρ is almost negligible in the case of the MCO, except for very low ρ values. Additionally, we show an example of the combination of the proposed constellations with channel coding, which is common practice in wireless communications standards, so the BER performance can be significantly improved. The chosen coding scheme is a 1/2-rate low density parity check code (LDPC) with a block of 8424 bits, which is used in 5G [1], and the performance is improved by about two orders of magnitude. In Fig. 8, we provide the average BER vs. the number of antennas (R); again, EEP has an error floor irrespective of the number of antennas, GAO outperforms EEP and MCO outperforms both GAO and EEP. In this case, the black crosses show the BER obtained when MCO is trained for the same ρ and R is set to values different from the one used for the optimization. Additionally, the effect of R is considerable when its value is relatively large, contrary to what happened with the SNR. In any case, these results demonstrate that it is feasible to use the constellation design for a particular ρ and/or R and for a wide range of operational values without additional offline training.

If we do not restrict β_u values ($\alpha_2 = 0$) in the objective function of GAO and MCO, the obtained solution is the same as given by Type B in [8]. Furthermore, if we set $\alpha_1 \approx \alpha_2$, GAO and MCO provide different solutions than the previous ones. In this case, the constellations of user 1 and user 2 will be equal to the ones in the top-center constellation in Fig. 4, while the constellation of the third user will be a classical QPSK. For this configuration, two different solutions were found, depending on how α_1 and α_2 were set, one with power terms $\beta_1 = \beta_2 = 1$ and $\beta_3 = 2.53$ and the other one with $\beta_1 = \beta_2 = \sqrt{10}$ and $\beta_3 = 1$. In both cases, the joint constellation resembles a 64-QAM constellation. We do not show the BER performance due to space constraints. The results for the multiuser scenario show an error floor caused

by the interference between users. Thus, we recommend to restrict the operational values to $\prod_{u=1}^{U} M_u \leq 64$ (Table II).

3) Scenario with $U = 2$, $M_u = 8$ and $\beta_u = 1$, $\forall u$: We set two UEs and a constellation size of $M_u = 8$. The results provided by MCO are obtained for $R = 300$ and SNR = 0 dB. In Fig. 9, we show the individual (top) and joint constellations (bottom) obtained with EEP, GAO and MCO (left to right). In this case, the constellations obtained with GAO and MCO are virtually the same, with the MCO being a rotated version of that of the GAO. For the case of EEP, the distance of the joint-symbols placed at the inner circle is very low, increasing the average BER. On the contrary, both GAO and MCO try to keep the same distance among the neighbour joint-symbols. The bit mapping policies are different, as observed from Fig. 9b and Fig. 9c, but the performance is the same, since several bit mapping policies are equivalent, due to the symmetry of the constellations.

Moreover, $M_u > 8$ can be performed with GAO and MCO, and the results follow the same strategy as for $M_u = 4$ and $M_u = 8$. However, their BER performance is degraded since the distance among joint-symbols is reduced.

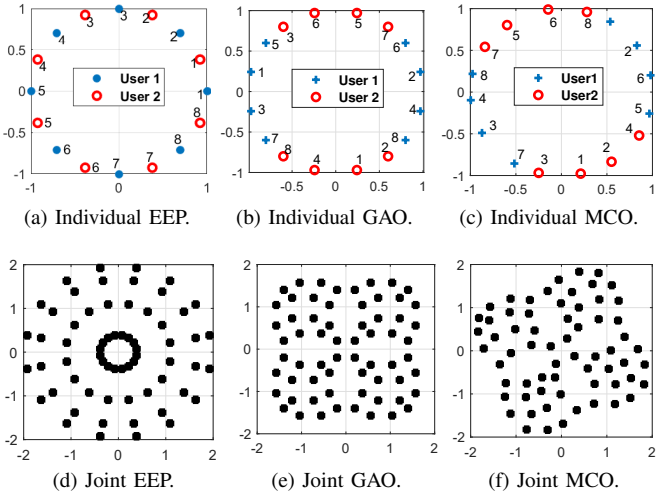

(a) Individual EEP. (b) Individual GAO. (c) Individual MCO.

(d) Joint EEP. (e) Joint GAO. (f) Joint MCO.

Fig. 9. Constellations for 2 users with 8 symbols per user with $\beta_u = 1$, $\forall u$.

We do not show a BER comparison for this scenario for space economy. Nevertheless, we can indicate that the improvement of the BER with R and the ρ for EEP is lower than that for GAO and MCO. This is caused by the reduced distance in the inner circle of the joint constellation. GAO and MCO have the same performance and both outperform EEP.

4) Scenario with $U = 4$ and $U = 5$ for $M_u = 2$ $\forall u$: In this scenario, we simulate 4 and 5 users, all with BPSK and $\beta_u = 1$, for the EEP and the proposed constellations in Table II (obtained with S3). The results shown in Fig. 10 are obtained for $R = 1000$ for both an IID Rayleigh channel and a standard geometric wideband (GEO) channel defined in TR 38.901 3GPP. The EEP is clearly outperformed by our proposal.

5) Scenario with $U = 3$ with different constellation sizes: In this case, we set 3 UEs with different constellation sizes (BPSK for the first user, and QPSK for the other two), to show that both GAO and MCO can cope with this type of

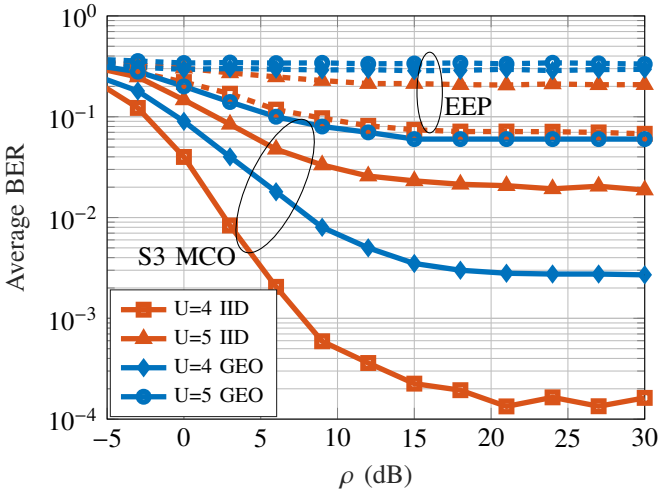

Fig. 10. BER vs. ρ for 4 and 5 users and 2 symbols per user with $\beta_u = 1$, for $R = 400$, for an IID and a GEO 3GPP channel. Continuous line for S3 MCO and dashed for EEP.

constraints. EEP is limited to having the same constellation sizes for all UEs. In Fig. 11, the individual constellations are shown on top, and the joint constellations are shown at the bottom. From left to right, we have the solution of the GAO for $\beta_u = 1$, $\forall u$, the MCO for $\beta_u = 1$, u and both the GAO and MCO for $\boldsymbol{\beta} = [1, 2, 2.4]$, which were the received powers obtained for $\alpha_1 \approx \alpha_2$. The BER performance is better for the MCO than for the GAO with $\beta_u = 1$, u, and the solution with $\boldsymbol{\beta} = [1, 2, 2.4]$ outperforms the other. Nevertheless, the BER performance is not added for space economy.

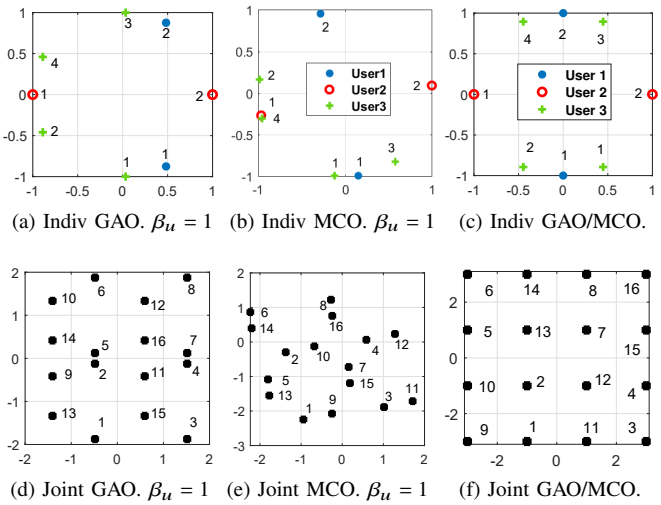

(a) Indiv GAO. $\beta_u = 1$ (b) Indiv MCO. $\beta_u = 1$ (c) Indiv GAO/MCO.

(d) Joint GAO. $\beta_u = 1$ (e) Joint MCO. $\beta_u = 1$ (f) Joint GAO/MCO.

Fig. 11. Constellations for 3 users with $M = [2, 2, 4]$. The results in the right are obtained with $\boldsymbol{\beta} = [1, 2, 2.4]$

B. Complexity of the Offline Optimization

The constellations proposed in Section VI-A have been obtained with the parameterization in Table III. For strategy S2, we indicate the cycle and step as (cycle-step). The total complexity is decreased by around 3 times for S2 with respect

to the strategy S1, but the total number of generations is greater and the total population size is similar. The solutions obtained for the S1, S2, S3 and S4 strategies are virtually identical and their differences manifest mainly in rotations and very small variations in the position of the symbols. The variables of both GAO and MCO S1 have been randomly initialized.

TABLE III
CONFIGURATION OF N_G, N_P, N_r AND N_s FOR DIFFERENT STRATEGIES.

	N_G	N_P	N_r	N_s
GAO 1st	$4(U+\sum M_u)$	$20(U+\sum M_u)$	X	X
GAO 2nd	30	300	X	X
MCO S1	$6(U+\sum M_u)$	$20(U+\sum M_u)$	1000	1000
MCO S2 (1-1)	$2(U+\sum M_u)$	$5(U+\sum M_u)$	100	100
MCO S2 (1-2)	$2(U+\sum M_u)$	$5(U+\sum M_u)$	100	100
MCO S2 (2)	$3(U+\sum M_u)$	$10(U+\sum M_u)$	1000	1000
MCO S4	$U+\sum M_u$	$U+\sum M_u$	1000	1000

As the previous results evidence, MCO has the best performance, outperforming the existing solutions and GAO, at the expense of increasing the complexity. In Section V, four different strategies were introduced to reduce the complexity, while obtaining the same results. In Table IV, we provide the total number of operations and execution time per design technique and strategy. GAO (1) and GAO (2) refer to the first and second step of GAO, respectively. All times are obtained for a processor AMD Ryzen 7 2700X 3.7 GHz. GAO uses a single processor and MCO uses parallel processors (12 times faster). Nevertheless, GAO performs on average around 10k operations per second and MCO around 150k operations per second per processor (as per Matlab matrix multiplication).

C. Non-coherent versus Coherent Scheme Performance

In this subsection, we consider a multipath time-varyimg channel and an implementation with OFDM modulation according to the 5G new radio numerology. To obtain the results, the coherence time is calculated as $T_c = 0.15 f_D^{-1}$ [31], where f_D is the maximum Doppler frequency. To implement time correlation effects we use the autocorrelation model of (2) in [32]. We also consider that the duration of an OFDM symbol is the inverse of the separation between subcarriers $T_s = 1/\Delta_f$. We can obtain the ratio of coherence time to the OFDM symbol duration as $N_{CT} = T_c/T_s$, which is given in Table V for 5G scenarios with very high mobility at 500 km/h (maximum speed for 5G). Only the values that are compatible with the allowed combinations of carrier frequency (f_c) and subcarrier spacing (Δ_f) in the 5G standard are shown; otherwise they are marked with "-" in the table. The coherent scheme uses channel estimation based on zero-forcing with pilot symbol assisted modulation (PSAM), as done in [7].

The results are shown in Fig. 12 for different N_{CT} values and multipath channels with a delay spread ($\sigma_\tau < 1\mu$s), so the minimum coherence bandwidth is $B_c \approx 1/(5\sigma_\tau) = 200$ kHz. Performing the differential encoding of the NC scheme over the frequency domain [10] and following the 5G standard [1], 4 out of 14 OFDM symbols correspond to reference signals for each slot. The SNR (ρ) for the coherent scheme has been penalized as $10\rho/14$ due to the channel estimation overhead. For high ρ, the NC outperforms the coherent scheme except for $N_{CT} \geq 10$. For $N_{CT} \leq 5$, the NC outperforms the coherent scheme for all ρ values. Also, the NC outperforms the coherent counterpart in the low ρ regime even for large N_{CT}.

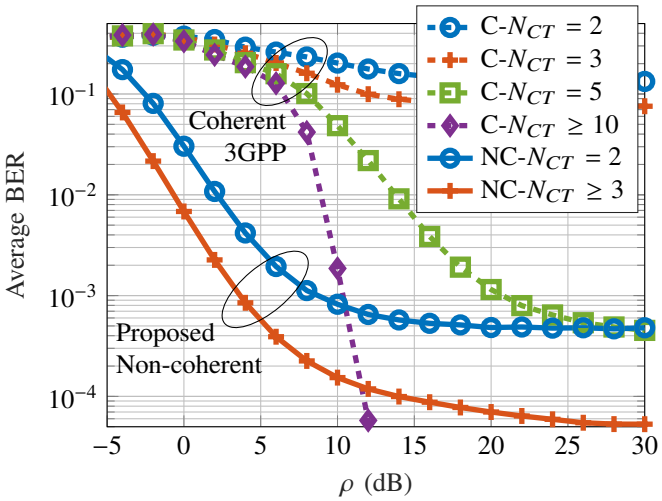

Fig. 12. Non-coherent (M_u = [4 4] and β_u = [1 1] from Table II) vs. coherent scheme (2 users with regular QPSK) for R=128, for different N_{CT}.

VIII. CONCLUSIONS

We have proposed new constellations using a novel technique based on evolutionary computation (EC) for the NC massive SIMO in multiuser UL scenarios. The proposed constellations outperform the state-of-the-art solutions.

We have shown that a classical analytical approach is intractable and proposed two different approaches for solving this problem, referred to as GAO and MCO. The former obtains the individual constellation and the bit mapping policy for each UE by solving two different optimization problems with a constrained complexity and considering assumptions about the PDF of the received joint-symbols. The latter determines the constellations and the bit mapping policies in a single optimization problem by evaluating the system BER using a Monte-Carlo simulation. The numerical results have verified our analysis of the distribution of the received joint-symbols, and shown that both GAO and MCO significantly outperform the existing constellations, in different channel types, while MCO outperforms GAO in most scenarios. It is thus corroborated that the proposed constellations work well in realistic channels and outperform the state-of-the-art. We have also presented the time complexity and number of operations for each scenario, confirming the validity of our complexity analysis.

This work contributes to the improvement of the performance of NC schemes combined with large number of antennas, with an offline design of the constellations. It has shown the viability of the proposed constellations to multiplex a moderate number of users with moderately large constellation sizes in the same time-frequency resources. This is a significant improvement with respect to previous NC constellations in the literature and paves the way to achieving even better multiplexing capabilities, particularly in scenarios where NC schemes outperform coherent ones.

TABLE IV
NUMBER OF PRODUCTS ($N_\times$) AND EXECUTION TIME (T) FOR DIFFERENT TECHNIQUES AND SCENARIOS ($N_\times \mid T$).

$N_\times$ | T	GAO (1)		GAO (2)		MCO S1		MCO S2		MCO S3		MCO S4	
U=2, M=[4 4]	$128{\cdot}10^3$	13s	$15.4{\cdot}10^3$	2.3s	$7.6{\cdot}10^{10}$	12h	$3.32{\cdot}10^{10}$	5h	$5{\cdot}10^8$	347s	-	352s
U=3, M=[4 4 4]	$1152{\cdot}10^3$	116s	$5.8{\cdot}10^3$	573s	$2.51{\cdot}10^{11}$	39h	$1.1{\cdot}10^{11}$	17h	$2{\cdot}10^9$	1231s	-	1302s
U=2, M=[8 8]	$1659{\cdot}10^3$	167s	$8.2{\cdot}10^9$	1.1h	$2.83{\cdot}10^{11}$	44h	$1.24{\cdot}10^{11}$	19h	$2.2{\cdot}10^9$	5003s	-	1315s
U=3, M=[2 2 4]	$155{\cdot}10^3$	16s	$2.56{\cdot}10^3$	0.7s	$9.2{\cdot}10^{10}$	14h	$4{\cdot}10^{10}$	6.2h	$8{\cdot}10^8$	367s	-	371s

TABLE V
RATIO OF T_c AND OFDM T_s (N_{CT}), FOR v = 500 KM/H FOR DIFFERENT CARRIER FREQUENCIES f_c IN GHZ AND CARRIER SPACING Δ_f IN KHZ.

N_{CT}	Δ_f = 15	Δ_f = 30	Δ_f = 60	Δ_f = 120	Δ_f = 240
f_c = 0.7	7	15	29	-	-
f_c = 3.6	1.4	2.8	5.6	-	-
f_c = 27	-	-	-	1.5	3
f_c = 54	-	-	-	-	1.5

REFERENCES

[1] *Physical Channels and Modulation (Release 15)*, 3GPP Std., 2018.

[2] P. Fan, J. Zhao, and C. I., "5G high mobility wireless communications: Challenges and solutions," *China Communications*, vol. 13, no. Supplement 2, pp. 1–13, Nov. 2016.

[3] Y. B. Zikria, S. W. Kim, M. K. Afzal, H. Wang, and M. H. Rehmani, "5G Mobile services and scenarios: Challenges and solutions," Oct. 2018.

[4] M. Chowdhury, A. Manolakos, and A. J. Goldsmith, "Coherent versus noncoherent massive SIMO systems: Which has better performance?" in *Proc. IEEE ICC*, June 2015, pp. 1691–1696.

[5] C. Wang, E. K. S. Au, R. D. Murch, W. H. Mow, R. S. Cheng, and V. Lau, "On the performance of the MIMO zero-forcing receiver in the presence of channel estimation error," *IEEE Trans. Wireless Commun.*, vol. 6, no. 3, pp. 805–810, Mar. 2007.

[6] L. Lu, G. Y. Li, A. L. Swindlehurst, A. Ashikhmin, and R. Zhang, "An overview of massive MIMO: Benefits and challenges," *IEEE J. Sel. Topics Signal Process.*, vol. 8, no. 5, pp. 742–758, April 2014.

[7] M. J. Lopez-Morales, K. Chen-Hu, and A. Garcia-Armada, "Differential data-aided channel estimation for up-link massive SIMO-OFDM," *IEEE Open J. Commun. Soc.*, vol. 1, pp. 976–989, July 2020.

[8] A. G. Armada and L. Hanzo, "A non-coherent multi-user large scale SIMO system relaying on M-ary DPSK," in *Proc. IEEE ICC*, June 2015, pp. 2517–2522.

[9] V. M. Baeza, A. G. Armada, W. Zhang, M. El-Hajjar, and L. Hanzo, "A noncoherent multiuser large-scale SIMO system relying on M-ary DPSK and BICM-ID," *IEEE Trans. Veh. Technol.*, vol. 67, no. 2, pp. 1809–1814, Feb. 2018.

[10] K. Chen-Hu and A. G. Armada, "Non-coherent multiuser massive MIMO-OFDM with differential modulation," in *Proc. IEEE ICC*, May 2019, pp. 1–6.

[11] S. Bucher, G. Yammine, R. F. H. Fischer, and C. Waldschmidt, "A noncoherent massive MIMO system employing beamspace techniques," *IEEE Trans. Veh. Technol.*, vol. 68, no. 11, pp. 11 052–11 063, Nov. 2019.

[12] S. Bucher and C. Waldschmidt, "Advanced Noncoherent Detection in Massive MIMO Systems via Digital Beamspace Preprocessing," in *Telecom*, vol. 1, no. 3. Multidisciplinary Digital Publishing Institute, 2020, pp. 211–227.

[13] S. Li, J. Zhang, and X. Mu, "Design of optimal noncoherent constellations for SIMO systems," *IEEE Trans. Commun.*, vol. 67, no. 8, pp. 5706–5720, Aug. 2019.

[14] H. Xie, W. Xu, W. Xiang, K. Shao, and S. Xu, "Non-coherent massive SIMO systems in ISI channels: Constellation design and performance analysis," *IEEE Syst. J.*, vol. 13, no. 3, p. 2252–2263, Sept. 2019.

[15] A. N. Sloss and S. Gustafson, "2019 Evolutionary algorithms review," *arXiv preprint arXiv:1906.08870*, 2019.

[16] H. Q. Ngo, E. G. Larsson, and T. L. Marzetta, "Energy and spectral efficiency of very large multiuser MIMO systems," *IEEE Trans. Commun.*, vol. 61, no. 4, pp. 1436–1449, April 2013.

[17] V. M. Baeza and A. G. Armada, "Non-coherent massive SIMO system based on M-DPSK for rician channels," *IEEE Trans. Veh. Technol.*, vol. 68, no. 3, pp. 2413–2426, March 2019.

[18] G. Cui, X. Yu, S. Iommelli, and L. Kong, "Exact Distribution for the Product of Two Correlated Gaussian Random Variables," *IEEE Signal Process. Lett.*, vol. 23, no. 11, pp. 1662–1666, 2016.

[19] Z.-H. Yang and Y.-M. Chu, "On approximating the modified Bessel function of the second kind," *Journal of inequalities and applications*, vol. 2017, no. 1, pp. 1–8, 2017.

[20] C. Walck, "Hand-book on statistical distributions for experimentalists," *University of Stockholm*, vol. 10, Sep. 2007.

[21] N. O'Donoughue and J. M. F. Moura, "On the product of independent complex Gaussians," *IEEE Trans. Signal Process.*, vol. 60, no. 3, pp. 1050–1063, Mar. 2012.

[22] X. Qi and F. Palmieri, "Theoretical analysis of evolutionary algorithms with an infinite population size in continuous space. Part I: Basic properties of selection and mutation," *IEEE Trans. Neural Netw.*, vol. 5, no. 1, pp. 102–119, 1994.

[23] M. Srinivas and L. Patnaik, "Genetic algorithms: a survey," *Computer*, vol. 27, no. 6, pp. 17–26, 1994.

[24] K. N. Pappi, N. D. Chatzidiamantis, and G. K. Karagiannidis, "Error performance of multidimensional lattice constellations—Part I: A parallelotope geometry based approach for the AWGN channel," *IEEE Trans. Commun.*, vol. 61, no. 3, pp. 1088–1098, Mar. 2013.

[25] Proakis, *Digital Communications 5th Edition*. McGraw Hill, 2007.

[26] Y. Gao, "Population size and sampling complexity in genetic algorithms," in *Proc. of the Bird of a Feather Workshops*, 2003, pp. 178–181.

[27] M. S. Gibbs, H. R. Maier, G. C. Dandy, and J. B. Nixon, "Minimum number of generations required for convergence of genetic algorithms," in *Proc. 2006 IEEE ICEC*, July 2006, pp. 565–572.

[28] J. Alander, "On optimal population size of genetic algorithms," in *Proc. CSSE*. IEEE Comp. Society, 1992, pp. 65–70.

[29] P. S. Oliveto, J. He, and X. Yao, "Time complexity of evolutionary algorithms for combinatorial optimization: A decade of results," *Intern. J. of Automat. and Comp.*, vol. 4, no. 3, pp. 281–293, 2007.

[30] J. Zhang, L. Zhu, Z. Xiao, X. Cao, D. O. Wu, and X. Xia, "Optimal and sub-optimal uplink NOMA: Joint user grouping, decoding order, and power control," *IEEE Wireless Commun. Lett.*, vol. 9, no. 2, pp. 254–257, Feb. 2020.

[31] T. S. Rappaport *et al.*, *Wireless Communications: Principles and Practice*. Prentice hall PTR New Jersey, 1996, vol. 2.

[32] K. E. Baddour and N. C. Beaulieu, "Autoregressive modeling for fading channel simulation," *IEEE Trans. Wireless Commun.*, vol. 4, no. 4, pp. 1650–1662, July 2005.

Manuel J. Lopez-Morales (S'18-GS'21-M'22) received the B.Eng. degree in Electrical Engineering from the Polytechnic University of Madrid in 2015 and the double M.Sc. degree in Telecommunications Engineering and Wireless Communications from the Polytechnic University of Madrid and Lund University, respectively, in 2018, both with Honors. He is currently an MSCA Ph.D. Student in the TeamUp5G project and is working towards the Ph.D. degree at the Universidad Carlos III de Madrid. He has been a visiting student in the Microwave Vision Group in Satimo (Italy) in 2014, in the Tokyo Institute of Technology (Japan) in 2016, in Ericsson AB (Sweden) in 2017, in the ISAE Supaero (France) in 2018, in Telefonica R&D (Spain) in 2020, in UNL Lisbon (Portugal) in 2021 and Nokia Spain in 2022. His research interests include antenna technology, signal processing, massive MIMO and wireless communications.

Kun Chen-Hu (S'16-GS'20-M'21) received his Ph.D. degree in Multimedia and Communications in 2019 from Universidad Carlos III de Madrid (Spain). Currently, he is a post-doctoral researcher in the same institution. He was awarded by UC3M in 2019 recognizing his outstanding professional career after graduation. He visited Eurecom (France) and Vodafone Chair TU Dresden (Germany), both as guest researchers. He also participated in different research projects in collaboration with several top companies in the area of mobile communications. He is the Web Chair for Globecom 2021, Madid (Spain), and online content editor for IEEE ComSoc. His research interests are related to signal processing techniques, such as waveforms design, reconfigurable intelligent surfaces, non-coherent massive MIMO and channel estimation.

Ana Garcia-Armada (S'96–A'98–M'00–SM'08) is a Professor at Universidad Carlos III de Madrid (UC3M), Spain. She has been a visiting scholar at Stanford University, Bell Labs, and University of Southampton. She has published more than 200 papers in conferences and journals and she holds five patents. She serves on the editorial boards of IEEE Transactions on Communications, IEEE Open Journal of the Communications Society and ITU Journal on Future and Evolving Technologies. She has been a member of the organizing committee of several conferences, including IEEE Globecom 2021 as the General Chair. She has received several awards from UC3M, the third place Bell Labs Prize 2014, the outstanding service award from the IEEE ComSoc Signal Processing and Communications Electronics technical committee and the outstanding service award from the IEEE ComSoc Women in Communications Engineering standing committee. Her research mainly focuses on signal processing applied to wireless communications.

Octavia A. Dobre (M'05–SM'07–F'20) received the Dipl. Ing. and Ph.D. degrees from the Polytechnic Institute of Bucharest, Romania, in 1991 and 2000, respectively. Between 2002 and 2005, she was with New Jersey Institute of Technology, USA. In 2005, she joined Memorial University, Canada, where she is currently a Professor and Research Chair. She was a Visiting Professor with Massachusetts Institute of Technology, USA and Université de Bretagne Occidentale, France. Her research interests encompass wireless communication and networking technologies, as well as optical and underwater communications. She has (co-)authored over 400 refereed papers in these areas. Dr. Dobre serves as the Director of Journals of the Communications Society. She was the inaugural Editor-in-Chief (EiC) of the IEEE Open Journal of the Communications Society and the EiC of the IEEE Communications Letters. She also served as General Chair, Technical Program Co-Chair, Tutorial Co-Chair, and Technical Co-Chair of symposia at numerous conferences. Dr. Dobre was a Fulbright Scholar, Royal Society Scholar, and Distinguished Lecturer of the IEEE Communications Society. She obtained Best Paper Awards at various conferences, including IEEE ICC, IEEE Globecom, IEEE WCNC, and IEEE PIMRC. Dr. Dobre is an elected member of the European Academy of Sciences and Arts, a Fellow of the Engineering Institute of Canada, and a Fellow of the Canadian Academy of Engineering.